# Vibration Powered RF-Transponder for Sensing Low Frequency Motion Events

**S K Gupta, V Pinrod, S Nadig, B Davaji and A Lal**

SonicMEMS Laboratory, School of Electrical & Computer Engineering, Cornell University, Ithaca, NY, USA

E-mail: skg73@cornell.edu

**Abstract**. Vibration energy harvesting offers a pathway to developing battery-less sensing solutions to be deployed in wireless sensor network nodes. The integration of the energy harvesters require regulation by power conditioning and control circuitry that consume some of the energy generated, reducing the effective energy available for node function. By designing a unique 3D-printed plastic structure for low frequency sensitivity and mechanical switching, and a lateral PZT bimorph for capturing energy from environmental vibrations, we report a zero-power consumption RF-transponder capable of detecting and reporting motion events without a battery. We have successfully picked up wireless transmissions on an external receiver placed ~25cm away from the transponder, shaken at 0.75 g and 20 Hz. We have additionally demonstrated the ability to harvest energy from 5 Hz vibrations up to just under 150 Hz. When placed on an oil-based electric generator, which vibrates when operating, the RF-transponder has successfully picked up the differing harmonics to identify the mode of operation as the economy or regular power setting.

## 1. Introduction

There is a need for reliable, battery-less, motion event detectors. Such devices are useful for detecting early vibrations on pipes that can lead to sudden implosions, fall events from hospital patients, excessive vibration of operating machinery, etc. [1]. While the power available to a vibration energy harvester is inversely proportional to frequency [2], these harvesters must be large to remain effective at low frequencies [3]. Frequency up-conversion is one remedy [4]. Because the power harvested is typically small, the power consumption of associated circuitry for node integration and transmitters can be detrimental to device utility. Our group has demonstrated up-conversion energy harvesting from a radioisotope source with a self-reciprocating actuator and switch [5]. He *et al.* [6] reported a sensor architecture using a mechanical switching mechanism that eliminated associated circuitry. The electromagnetic harvester directly drove the antenna, primed only by the voltage output of the sensor. Jiang *et al.* [7] removed the need for a priming voltage with a 75x27x25 $mm^3$ design. Additionally, 3D-printing has been shown useful in housing energy harvesters [8]. We report a novel apparatus of a compact 3D-printed structure that exploits a mainly lateral serpentine design to excite the impulse response of a piezoelectric lateral bimorph, providing multiple resonant peaks at frequencies ranging from 5 Hz to under 150 Hz. Lateral structures presented in this work have the potential of providing a thin overall package needed for convenient attachment to two-dimensional surfaces. The mechanical switching mechanism eliminates the need for CMOS ICs needed in more conventional approaches.

## 2. Device Concept

A piezoelectric lateral bimorph [9] is anchored on top of a 3D-printed plastic structure (figure 1). The structure consists of a proof mass connected to a fixed frame through a serpentine spring providing it with substantial motion at low-frequencies from near zero to under 150 Hz. Figure 2 illustrates the sequence of events leading to RF transmission. When vibrating, the plastic proof mass and mounted bimorph collide with the 3D-printed structure's frame, inducing the impulse response of the piezoelectric energy harvester. The induced electrical charge is rectified and stored onto a capacitor. An integrated contact switch closes after the spring induces the impulse, triggering the LC tank oscillations and RF pulses that can be detected using a tuned radio. Since the contact switch only closes upon sufficient amplitude of motion, the switch gap can be adjusted so that it only switches upon a desired threshold of motion, or event. By using a sufficiently small capacitor, the time it takes for the contact to close will be significantly longer than the charge time of the capacitor. This will ensure the capacitor is fully charged before transmission.

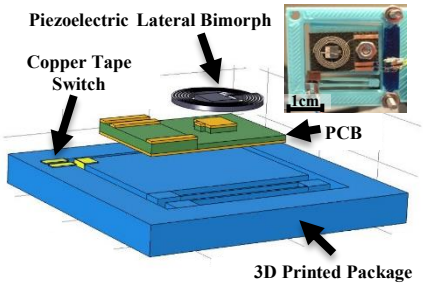


**Figure 1.** Assembly of transponder. Inset: Photograph of fabricated

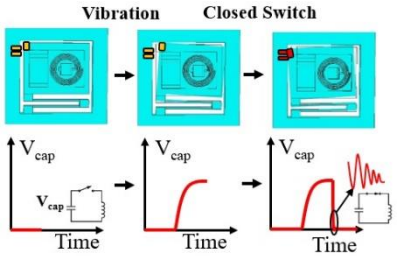


**Figure 2.** The capacitor charges as the proof-mass hits one side of the frame and discharges as it hits the other.

## 3. Device Model

Both electrical and mechanical processes define the system. The RF-transponder can be represented as the combination of the equivalent circuit and mechanical system model shown in figure 3.

### *3.1. Equivalent Circuit*

The electrical model for a piezoelectric energy harvester (*EH*) has already been shown to be a current source with a shunt capacitor and resistor [10]. The current source, *i(x)*, is dependent on the displacement of the bimorph, *x*. The charge from the piezoelectric is then rectified using the configuration presented in [11]. The rectified charge is stored onto a capacitor ($C_s$) which connects to an inductor (*L*) through the contact switch (*SW*).

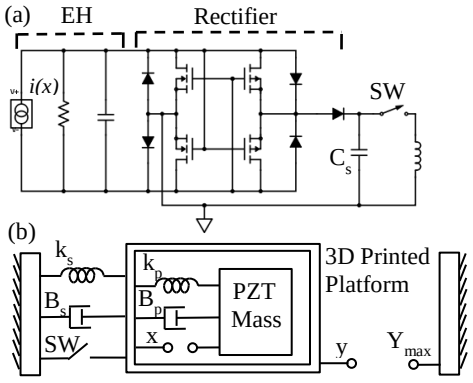


**Figure 3.** Electrical and mechanical model.

### *3.2. Mechanical Model*

The RF-transponder consists of two spring-mass systems. The 3D-printed structure is anchored on one side with a spring constant ($k_s$), damping force ($B_s$) for the stage, electro-mechanical switch (*SW*) and mass ($m_{\text{total}}$). On top of the proof mass, the second spring-mass system is defined by the piezoelectric bimorph. It too has an associated spring constant ($k_p$), a damping force ($B_p$) and mass ($m_p$). The displacement of the piezoelectric and 3D-printed platform is represented by *x* and *y* respectively. The damping of the piezoelectric is the mechanism of energy extraction and so defines the upper boundary of power generation [12]. The 3D-printed platform is a driven harmonic oscillator with displacement amplitude ($|Y_0|$) in response to an acceleration ($a_{in}$). For maximum power transfer, we consider the case where the 3D-printed package is excited at its resonance ($\omega_0$):

$$|Y_0| = a_{in}\left((\omega_0^2 - \omega^2)^2 + \frac{B_s^2}{m_{total}^2}\omega^2\right)^{-\frac{1}{2}} = \frac{a_{in}m_{total}}{B_s\omega_0} \quad (1)$$

The model has two cases defined by whether the proof mass hits the surrounding frame (gap of $Y_{max}$).

*3.2.1. Case one:* $|Y_0| < Y_{max}$. The maximum power achievable is calculated in [12] where the stage and drive resonance frequencies ($\omega_0$) are much less than the bimorph structure resonant frequency ($\omega_n$):

$$P_{max} = \frac{Y_0^2 \omega_0^5 m_p}{4\omega_n^2}\left|\frac{\omega_0^2}{\omega_n^2} - 1\right|^{-1} \approx \frac{a_{in}^2 \omega_0^3 m_{total}^2 m_p}{4\omega_n^2 B_s^2}, \qquad a_{in} < \frac{Y_{max} B_s \omega_0}{m_{total}} \tag{2}$$

Here we have assumed that the damping of the PZT is much less than the damping of the stage.

*3.2.2. Case two:* $|Y_0| = Y_{max}$. In this case, the proof mass will hit the sidewall and induce the bimorph impulse response. The bimorph is a damped harmonic oscillator that experiences a jump in velocity due to its momentum before collision. We assume a perfectly elastic collision where all the momentum from the bimorph and plastic platform remain in their respective systems at time $t_i$ where $y(t_i) = Y_{max}$:

$$\dot{x}(t_i) = \frac{a_{in} m_{total}}{B_s} \cos\left(\sin^{-1}\left(\frac{Y_{max} B_s \omega_0}{a_{in} m_{total}}\right)\right) \tag{3}$$

Because the piezoelectric is driven well below its resonant frequency before impact, $x(t_i) \approx 0$ relative to the displacement caused after collision. Thus, the solution to the damped harmonic oscillator is:

$$x(t) = \frac{\dot{x}(t_i)}{\omega_1}\exp\left(-\frac{B_p(t-t_i)}{2m_p}\right)\sin(\omega_1(t-t_i)), \qquad \omega_1 = \left(\omega_n^2 - \frac{B_p^2}{4m_p^2}\right)^{\frac{1}{2}}, \qquad t > t_i \tag{4}$$

The maximum mechanical power harvestable by the piezoelectric at time $t$ after the impulse is then:

$$P(t) = B_p \dot{x}^2(t), \qquad P(t_i) = B_p \frac{a_{in}^2 m_{total}^2}{B_s^2}\cos^2\left(\sin^{-1}\left(\frac{Y_{max} B_s \omega_0}{a_{in} m_{total}}\right)\right) \tag{5}$$

Figure 4 shows the maximum mechanical power of the bimorph for a device with the net effective mass 1 gram for different accelerations. The power is determined by the ratio of the bimorph damping factor over the 3D-printed structure's damping factor squared. We need an additional derivation to convert this mechanical power into electrical power. The energy harvested can be optimized by minimizing the damping of the 3D-printed structure relative to the lateral bimorph.

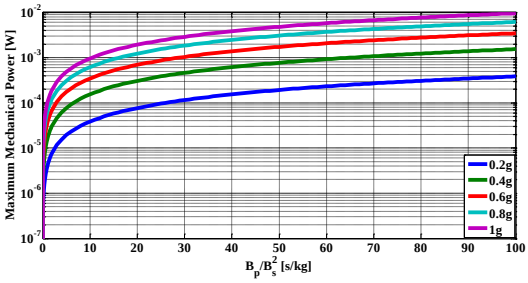


**Figure 4.** Maximum mechanical power of bimorph over different accelerations as a function of damping ratio. $m_{total}$ = 1 gram.

## 4. Device Fabrication and Testing

The PZT lateral bimorph [9] with two-axis sensitivity uses a compact spiral design shown in figure 5 to decrease the required area and increase in-plane symmetry. An additional groove cut is added along the middle of the spiral bimorph to increase out-of-plane sensitivity, providing full three-axis sensitivity for all angle energy harvesting. The bimorph is fabricated by selective scanning of the LPFK Protolaser U, allowing a simple, single step process for achieving a smooth circular geometry that is otherwise challenging with other processes. The plastic spring-mass of thickness 3 mm is 3D-printed from a MakerBot Desktop. The serpentine spring segments have lateral

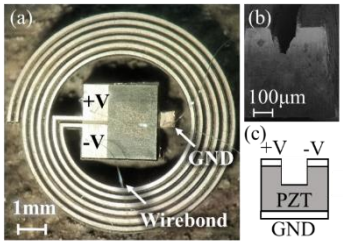


**Figure 5.** Photograph, SEM and schematic of bimorph and cross section

dimension 15.5x0.3 mm$^2$ and 2x2.5 mm$^2$. The proof mass has an area of 18x14 mm$^2$ and the inertial frame has inner dimensions of 20x20 mm$^2$ with a 4 mm width. Holes with a 2 mm diameter are included for mounting purposes.

The 3D-printed spring-mass structure has a resonance frequency of 24 Hz, a Q factor of 17 and spring constant of ~66 N/m. The PZT bimorph has a resonance frequency of 416 Hz, a Q factor of 173.5, an output capacitance of ~0.2nF and spring constant of ~653 N/m. This gives a maximum achievable power of ~1.9 nW just before collision and ~11 mW/g$^2$ after collision when excited at resonance.

The RF-transponder was mounted on a tilt to a shaker table to measure the voltage induced on the bimorph for accelerations. A small magnetic ball mass was added to the proof mass to further increase the output of the system. The results are shown in figure 6a. It should be noted that the 1 MΩ load was not optimized for maximum power transfer. Figure 6b shows a wireless transmission in the 20-100 MHZ range picked up by an LC tank 9 inches from the transponder. Figure 7 shows the bimorph captured different motion signatures when placed on a generator.

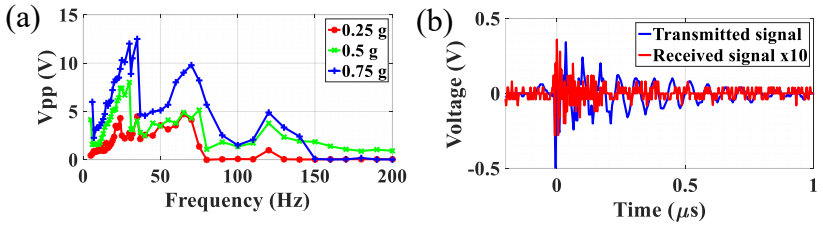


**Figure 6.** Frequency response of bimorph and transmission of transponder excited at 20 Hz and 0.75g by a shaker table.

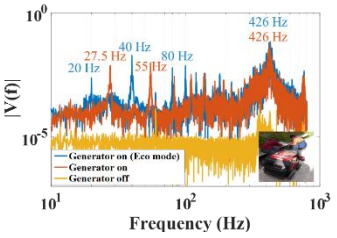


**Figure 7.** FFT of the bimorph output on the generator with modes of operation.

## 5. Conclusions

A RF-transponder has been built that transmits to an external RF receiver upon the onset of a motion event which is greater than a set motion threshold, without the use of any power conditioning circuitry, battery, control circuitry or external sensors. While a PZT lateral bimorph is used for capturing energy from vibrations, it can be swapped out with any type of energy harvesting device capable of converting the energy from impact into electrical energy. This device is applicable in wearables, industrial machinery, medical patient monitoring, intruder detection and automotive sensing.

## 6. Acknowledgements

This work was performed in part at the Cornell NanoScale Facility, a member of the National Nanotechnology Infrastructure Network, which is supported by the National Science Foundation (Grant ECCS-0335765). The SEM in figure 4b was taken by Leanna Pancoast. Funding for this project was provided by the DARPA NZERO and PASCAL programs.

## References

[1] Akyildiz I F, Su W, Sankarasubramaniam Y and Cayirci E 2002 **38** *Computer Networks* 393-422
[2] Roundy S, Wright P K and Rabaey J M 2004 *Energy Scavenging for Wireless Sensor Networks* (Boston: Kluwer Academic Publishers) pp 31-39
[3] Roundy S 2005 **16** *JIMSS* 809-23
[4] Ashraf K, Khir M H, Dennis J O and Baharuddin Z 2012 *Proc. PowerMEMS* (Atlanta, USA) pp 416-9
[5] Lal A, Duggirala R and Li H 2005 **4(1)** *IEEE Pervasive Computing* 53-61
Tin S and Lal A 2009 *Proc. IEEE IEDM* (Baltimore, USA) pp 539-42
[6] He C, Kiziroglou M E, Yates D C and Yeatman E M 2011 **11** *IEEE Sensors* 3437-45
[7] Jiang H, Kiziroglou M E, Yates D C and Yeatman E M 2015 **2** *IEEE IoT* 5-13
[8] Constantinou P and Roy S 2015 *Proc. PowerMEMS* (Boston, USA)
[9] Nadig S, Ardanuc S and Lal A 2015 *Proc. IEEE MEMS* (Estiril, Portugal) pp 1129-32
[10] Kiran S, Selvakumar D, Mervin J and Pasupuleti H 2015 *Proc. ICCEREC* (Bandung, Indonesia) pp 63-9
[11] Romani A, Filippi M, Dini M and Tartagni M 2015 **12** *ACM JETC* 7:1-17
[12] Mitcheson P D, Green T C, Yeatman E M and Holmes A S 2004 **13** *J MEMS* 429-40